Current Science
CS 5 (4), 4295-4304 (2025)
**Received 20 May** 2025 | **Revised 21 June** 2025 | **Accepted 25 July**. 2025 | **Online Available 31 August** 2025
https://doi.org/10.52845/CS/2025-5-4-75

**Current Science**
Current Science

**OPEN ACCESS**
**ISSN(O)2795-8639**

**Original Article**

# Sodium Dichloroacetate Alleviates Pulmonary Arterial Hypertension by Affecting Glycolysis through the HIF-A/ PDH-E1α Axis

**Qiuhong Chen[1], Jinchen He[1], Meiling Chen[1], Guoqu Jia[1], Rui Yin[1], Songjie Bi[1], Qi Wu[1]** ✉

**[1]Department of Cardiovascular Medicine, The Second Affiliated Hospital of Chengdu Medical College, Nuclear Industry 416 Hospital, Chengdu, 610000 Sichuan, China**

**[*]Corresponding Author: Qi Wu**

**Abstract:**

**Background:** Pulmonary arterial hypertension (PAH) is a progressive disease with limited therapeutic options. Based on the therapeutic effects of sodium dichloroacetate (DCA) on PAH, we aimed to explore the effects and potential mechanism of DCA in MCT-induced rat model of PAH.

**Methods:** The rat model of PAH was established by a single subcutaneous injection of monocrotaline (MCT)(60 mg/kg). Tirty male Sprague Dawley rats at the age of 6 weeks (150 g to 160 g) were randomized for five groups. Control group (normal saline 100 mg/kg i.p. daily), MCT group (normal saline 100 mg/kg i.p. daily), MCT+lactate group (lactate 500 mg/kg i.p. weekly), MCT+DCA group (DCA100 mg/kg i.p. daily), MCT+DCA+lactate group (DCA 100 mg/kg i.p. daily+lactate 500 mg/kg i.p. weekly), were administered from the 7th day after MCT injection. After 28th day, hemodynamic parameters, histological changes of the pulmonary arterial vessels and right ventricle (RV), glycolysis and lactate metabolism, the expression of H3K18la/HistoneH3, HIF-α and PDH-E1α were assessed.

**Results:** DCA attenuated MCT-induced PAH, with significant reductions in RV systolic pressure, pulmonary artery wall thickness and RV hypertrophy. DCA treatment alleviated significantly the glycolysis and lactate metabolism in MCT-induced PAH model rats. DCA treatment significantly reduced the expression of HIF-α, PDH-E1α, and the level of H3K18la/HistoneH3 in the MCT-induced PAH model rats.

**Conclusions:** DCA alleviates MCT-induced PAH, potentially by inhibiting the HIF-α/PDH-E1α axis, which leads to reduced glycolysis and subsequent histone H3K18 lactylation (H3K18la).

**Keywords: Pulmonary arterial hypertension, glucose metabolism, metabolic reprogramming, glycolysis**

## Introduction

Pulmonary arterial hypertension is a progressive life-threatening cardiopulmonary vascular disease involving various pathological mechanisms, including hypoxia, cellular metabolism, inflammation, abnormal proliferation and apoptosis. Specifically, metabolism has attracted the most attention. Glucose metabolism is essential to maintain the cardiopulmonary vascular function. In 1924, Warburg et al (1) observed an interesting phenomenon, in which tumor cells exhibited a preference for glycolysis to promote proliferation, regardless of the presence of sufficient oxygen. This phenomenon for energy supply that requires neither oxygen nor mitochondria is known as the 'Warburg effect' and is characterized by high glucose uptake, lactate secretion and anaerobic energy production(2). Similar to cancer, The Warburg effect is a contributing factor to PAH, as its characteristic features, such as high glucose uptake, lactate secretion, and anaerobic energy production, are associated with PAH (3, 4). Numerous studies have investigated the relationship between

abnormal glucose metabolism and development of PAH to facilitate its treatment.

During glycolysis, large amounts of lactate are produced as an energy source to maintain cellular metabolism. Histone lysine lactylation has been shown to be caused by lactate accumulation and regulated by lactate levels. The regulation of gene expression by lactate through histone lactylation modification is a newly discovered epigenetic modification, and a novel post-translational modification (PTM) has been identified in human and mouse core histones(5). Histone lactylation is involved in many cellular processes, including translation, metabolism, recombination, and repair (6). Mechanically, lactate is used as a substrate to generate lactyl-CoA for lysine lactylation on histones, a process that regulates gene expression in a variety of pathophysiological conditions(7). Meanwhile, in terms of transcription and antigenic variation, chromatin repression or induction is determined by the PTM status of core histones(8).

In addition to their critical function in signal transduction and cellular metabolism, PTMs also play a key role in regulating protein conformation, stability and function (6). Several factors were associated with pulmonary arterial smooth muscle cells (PASMCs) and pulmonary arterial endothelial cells (PAECs) proliferation, including lactate metabolism, oxidative stress response, hypoxia-inducible factor 1(HIF-1) pathway and PTMs. A number of studies have shown that glycolysis plays a critical role in PASMC proliferation, and inhibition of glycolysis can inhibit PASMC proliferation and migration and also reverse PAH in animal models (9). Chen et al. found that mROS-mediated HIF-1α-driven glycolysis promotes pulmonary artery remodeling. Mechanistically, lactate accumulation increases histone lactylation at HIF-1α targets linked to proliferative phenotype(10). Lactate serves as substrate of H3K18 lactylation, which is also accumulate in PAH lungs because of the hypoxic environment and the increase of Warburg effect. In conclusion, H3K18 lactylation is elevated in PAH, and promoted the progress of PAH.

Pyruvate dehydrogenase (PDH), as a critical multi-subunit enzyme, gates the entry of glucose-derived pyruvate into the the tricarboxylic acid (TCA) cycle, thereby acting as a negative regulator of glycolysis in most cell types. Dichloroacetate (DCA), an extensively studied pyruvate mimetic, works by inhibiting pyruvate dehydrogenase kinases（PDKs） by competitively binding to the variable configuration sites of PDK1-4(11). We hypothesized that DCA could alleviate PAH by inhibiting pathological glycolysis and subsequent H3K18 lactylation.

## Materials and Methods

### Animal Model and Treatment Plan

All animal experiments were conducted in the SPF animal room of the Central Laboratory of Chengdu Medical College. Tirty male Sprague Dawley rats at the age of 6 weeks (150 g to 160 g) were randomized for five groups : control group (blank control group, $n = 6$); MCT group ($n = 6$), where rats received intraperitoneal injections (i.p.) of MCT (60 mg/kg) from the 1th day to the 28th day(12, 13); MCT + Lactate group ($n = 6$), where rats received MCT (60 mg/kg) intraperitoneally on day 1 and Lactate (0.5g/kg/7d) administered intraperitoneally from day 7 to day 28; MCT + DCA group ($n = 6$), where rats received MCT (60 mg/kg) intraperitoneally on day 1 and DCA(100 mg/kg/d) administered intraperitoneally from day 7 to day 28; MCT + DCA+ Lactate group($n = 6$), where rats received MCT (60 mg/kg) intraperitoneally on day 1, Lactate (500 mg/kg/7d) and DCA(100 mg/kg/d) administered intraperitoneally from day 7 to day 28. On day 28, echocardiographic measurements were performed on all animals. The animal feeding conditions were (22±2) ℃, 21% $0_2$, and a light cycle of 12h: 12h. General purpose rats were fed synthetic feed and allowed to drink water freely. The rats were then euthanized under deep anesthesia (i.p. of 3% pentobarbital sodium, 100 mg/kg), and their heart and lung tissues were collected for further analysis(14).

Doppler echocardiography measurement

Doppler echocardiography was used to identify PAH on the 28th day of SD rats modeling. The Doppler echocardiography parameter "Pulmonary Artery Acceleration Time" (PAAT) is considered as an echocardiographic indicator of PAH(15), which is negatively correlated with the invasive measured mean pulmonary artery pressure (mPAP). Transthoracic echocardiography was performed using a Vivid E9 ultrasound system equipped with a 12-MHz transducer (GE Healthcare). The rats were anesthetized with an

i.p. injection of 3% sodium pentobarbital (40 mg/kg). PAAT was measured near the pulmonary valve on the left chest. According to the current guidelines of the American Society of Echocardiography, mPAP can be calculated according to the following formula: mPAP = 72-(0.42 × PAAT, PAAT < 120 ms)(14, 16). Following echocardiographic assessment, the rats were sacrificed under deep anesthesia (i.p. 3% pentobarbital sodium,100 mg/kg) (16), and the lung and heart tissues were collected for analysis. Echocardiographic data were analyzed using Echopac BT11 software (v.6.5; GE Healthcare).

**Right Ventricular Hypertrophy Measurement**

To evaluate the right ventricular hypertrophy index (RVHI), rats were sacrificed under deep anesthesia (i.p. 3% Pentobarbital Sodium, 100 mg / kg), and the heart tissue was collected and weighed. Atrium and external blood vessels were carefully removed from the isolated heart using 0.9% normal saline. The weights of both right ventricle (RV) and left ventricle (LV) plus septum (S) were recorded(12, 17). The RVHI was calculated by [RV/(LV + S)](18).

**H&E and Masson Staining**

After fixation in 4% paraformaldehyde for 48 h, the lung tissue was embedded in paraffin and cut into 5 μm tissue sections. H&E and Masson staining of paraffin-embedded sections of lung tissues were performed to evaluate pathologic changes and collagen fiber hyperplasia under light microscopy. The ratio of vascular wall thickness and the ratio of the vascular wall area in the middle and small arterioles with an outer diameter of 50–150 μm were measured by using an image analyzing system (Image-Pro Plus, Media Cybernetics, Silver Spring, MD, USA). Simultaneously, Pulmonary vascular remodeling was evaluated by the percentage of the thickness of the vessel wall (WT%), the percentage of the vessel wall area (WA%) and the percentage of vascular lumen area ( LA%). WT% = [2 × (blood vessel outer diameter-blood vessel inner diameter)] / (blood vessel outer diameter) × 100%; WA% = (total area of blood vessel-blood vessel Internal area) / total area of blood vessel × 100%; LA% = (blood vessel Internal area) / total area of blood vessel × 100% (19). For each animal, over 10 randomly chosen vessels that were nearly round or oval in shape were measured and averaged by an observer blinded to the experimental groups.

**Measurement of Lactate Levels**

The blood sample was collected from the heart at theend of the experiment to measure the amount of lactate. The levels of lactate were measured using ELISA kits according to the manufacturer's instructions.

**Western Blot Analysis**

For western blotting, after protein electrophoresis in each group, after separation with 10% SDS-PAGE, the target protein was transferred to PVDF membrane and blocked with 5% skim milk for 2 h. Proteins were incubated overnight at 4 °C with the following antibodies: anti-GAPDH (A19056, abclonal, China; 1:10,000), anti-MCT1 (bs-10249R, Bioss, China; 1:1000), anti-MCT4 ( sc-376140, Santa Cruz, USA; 1:1000), anti-HIF-α (sc-13515, Santa Cruz, USA; 1:1000), anti-PDH-E1α (bs-4034R, Bioss, China; 1:1000), anti-HistoneH3 (A17562, abclonal, China; 1:1000), anti-H3K18la ( A21214, Abcam; 1:1000). Horseradish peroxidase-labeled anti-mouse antibody or anti-rabbit antibody (abclonal, China; 1:1000) was used as the secondary antibody incubated at room temperature for 2 h. The membranes were visualized with enhanced chemiluminescence reagent (Thermo Science, Waltham, MA, USA) and Image J software (Bethesda, USA, National Institutes of Health) were used to quantize the grayscale values. Protein levels were normalized to GAPDH.

**Statistical Analysis**

Statistical software SPSS 20.0 and GraphPad Prism 8.0 were used to analyze the experimental results. All results were expressed as mean ± SD. Statistical comparisons One-way ANOVA followed by a post-hoc test. Probability values < 5% ($P < 0.05$) were considered significant.

**Results**

**Effects of DCA on cardiac function in MCT-induced PAH model rats.**

The efficacy of DCA in the treatment of PAH was evaluated by measuring mPAP and the cardiac-related indices, the efficacy of lactate in the treatment of PAH was evaluated by measuring mPAP and the cardiac-related indices. The mPAP

in the MCT group and MCT+Lactate group were significantly higher than that in the control group ($p < 0.01$); the mPAP in the MCT+Lactate group was significantly higher than that in the MCT group ($p < 0.01$). But the mPAP in the MCT+DCA group was significantly lower than that in the MCT group ($p < 0.01$); the mPAP in the MCT+Lactate+DCA group was significantly lower than that in the MCT+Lactate group ($p < 0.01$). (Fig. 1D)

MCT treatment led to significant increases in the cardiac-related indices (right ventricular hypertrophy index, right ventricular anterior wall thickness at diastole, right ventricular anterior wall diameter in diastole, right ventricular anterior wall thickness at systole and right ventricular anterior wall diameter in systole) compared with the control group ($p < 0.01$), indicating right ventricular hypertrophy. Meanwhile, lactate treatment exacerbated significantly right ventricular hypertrophy compared with the MCT group ($p < 0.01$). However, the cardiac-related indices in the MCT+DCA group was significantly lower than that in the MCT group ($p < 0.01$); the cardiac-related indices in the MCT+Lactate+DCA group was significantly lower than that in the MCT+Lactate group ($p < 0.01$), indicating DCA treatment alleviated right ventricular hypertrophy.(Fig. 1A, 1B, 1E, 1F,1G, 1H,1I)

Observed under a light microscope, the myocardial cells of MCT group and MCT+Lactate group were significantly hypertrophic, the intersections of myocardial fibers were enlarged, broken and disordered in arrangement, meanwhile, inflammatory cell infiltration could be observed compared with the control group. However, DCA treatment alleviated significantly morphology of cardiomyocytes in the MCT+DCA group and MCT+Lactate+DCA group compared with the MCT group and the MCT+Lactate group, respectively. (Fig. 1C).

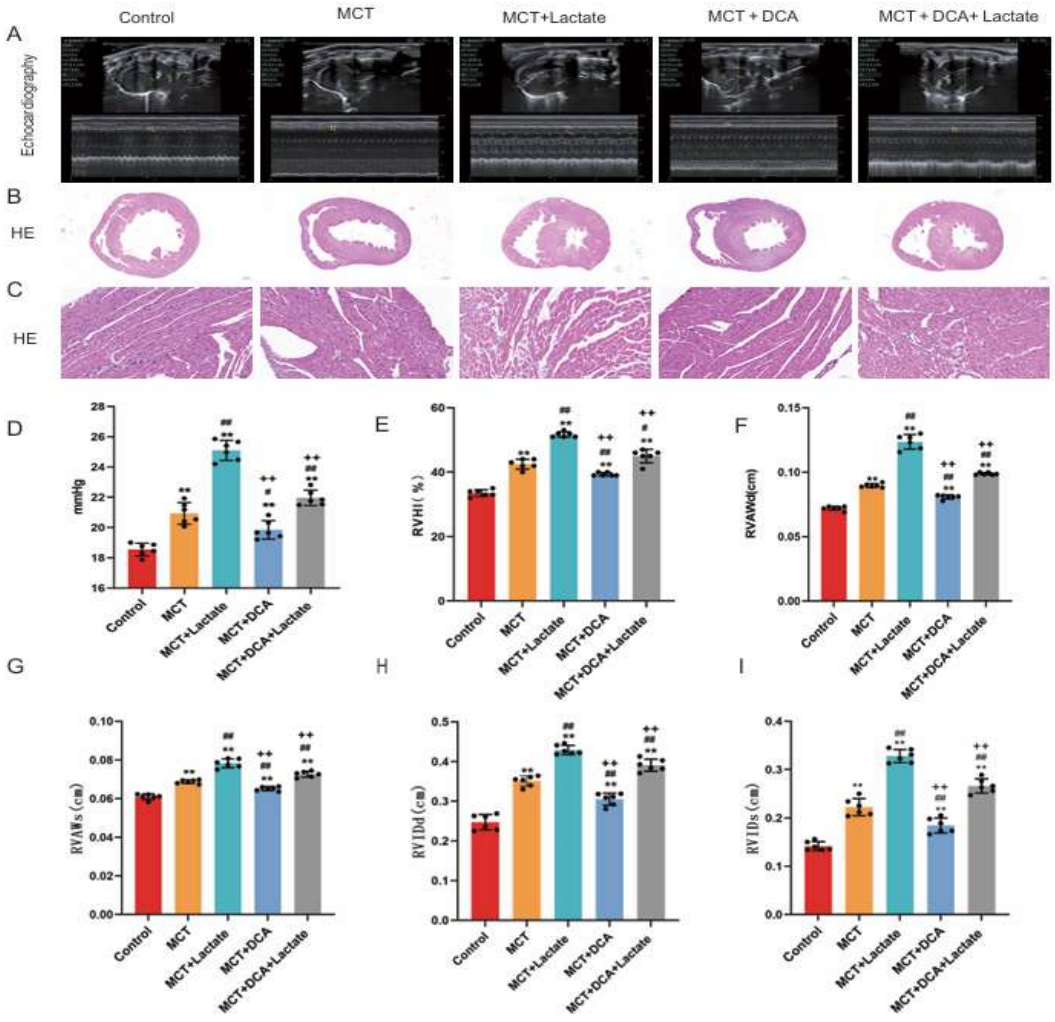


**Figure 1. (A) Structural changes in the right ventricle of the rats measured by ultrasound. (B) HE staining of the heart. (C) HE staining of myocardium. (D) mPAP quantitative analysis. (E) RVHI**

**quantitative analysis. (F) RVAWd quantitative analysis. (G) RVIDd quantitative analysis. (H) RVIDd quantitative analysis.(I) RVI Ds quantitative analysis. **$P$<0.01 vs. control. $^{\#\#}P$<0.01 vs. MCT. $^{++}P$<0.01 vs. MCT+Lactate; MCT: monocrotaline; mPAP, pulmonary arterial pressure; RVHI: right ventricular hypertrophy index; RVAWd: right ventricular anterior wall thickness at diastole; RVAWs: right ventricular anterior wall diameter in diastole; RVIDd: right ventricular anterior wall thickness at systole; RVIDs: right ventricular anterior wall diameter in systole.**

### Effects of DCA on the remodeling of pulmonary vascular in MCT-induced PAH model rats.

Pathological changes in pulmonary arteries in the MCT group included notable narrowing of vessel lumens and intima-media thickening along with marked arterial remodeling(Fig. 2A). WT% and WA% of MCT+DCA group and MCT+Lactate+DCA group alleviated significantly compared with the MCT group and the MCT+Lactate group, respectively ($p < 0.01$, Fig. 2B, 2C). Meanwhile, LA% of MCT+DCA group and MCT+Lactate+DCA group decreased significantly compared with the MCT group and the MCT+Lactate group, respectively ($p < 0.01$, Fig. 2D), indicating DCA treatment alleviated significantly pulmonary vascular remodeling. In addition, WT% and WA% of MCT+Lactate group higher significantly compared with the MCT group ($p < 0.01$, Fig. 2B, 2C), LA% of MCT+Lactate group increased significantly compared with the MCT group and the MCT group ($p < 0.01$, Fig. 2D), indicating lactate treatment led to significant increases in the pulmonary vascular remodeling.

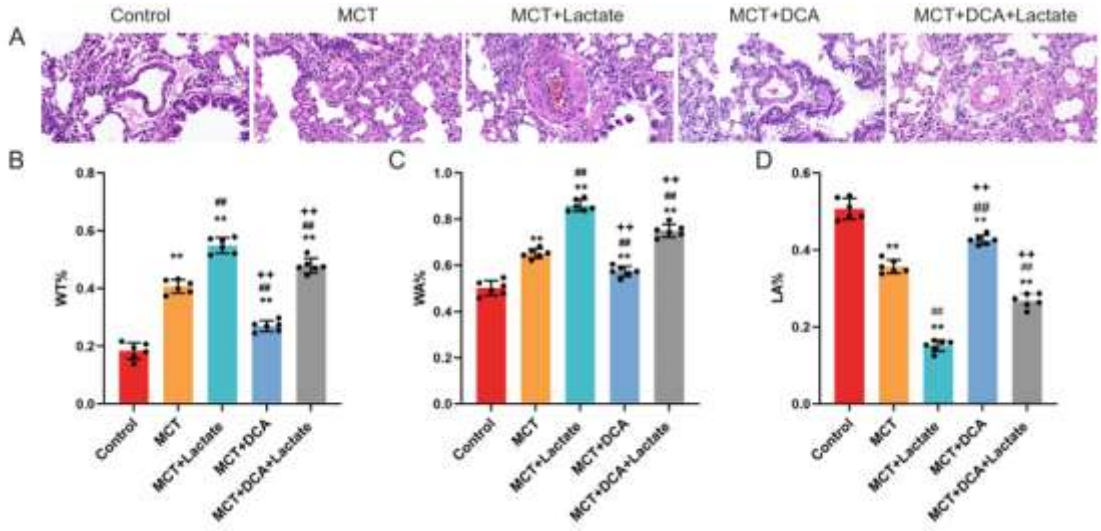


**Figure 2. (A) HE staining of the pulmonary artery. (B) WT quantitative analysis. (C) WT quantitative analysis. (D) LA quantitative analysis. **$P$<0.01 vs. control. $^{\#\#}P$<0.01 vs. MCT. $^{++}P$<0.01 vs. MCT+Lactate; MCT: monocrotaline; WT%: the percentage of vascular wall thickness; WA%: the percentage of vascular wall area; LA%: the percentage of vascular lumen area.**

### Effects of DCA on the glycolysis and lactate metabolism in MCT-induced PAH model rats.

Rather than entering the TCA cycle, pyruvate is converted into lactate by cytosolic lactate dehydrogenases (LDHs) in highly glycolytic cells of the PAH patients and animal models of PAH(20, 21). Finally, as a result of enhanced glycolysis, microenvironments become acidification with increased lactate production. Our latest research shows MCT treatment led to significant increases in the lactate levels compared with the control group ($p < 0.01$, Fig. 3B), the lactate levels of MCT+DCA group decreased significantly compared with the MCT group ($p < 0.01$, Fig. 3B). The export and uptake of lactate are dependent on monocarboxylate transporters (MCTs), MCT1 and MCT4 transport lactate across the cell membrane. MCT1 primarily mediates lactate influx, whereas MCT4 is responsible for lactate efflux. the expression of MCT1 and MCT4 were closely related to the degree of glycolysis(22). the expression of MCT1 and MCT4 in MCT+DCA group and

MCT+Lactate+DCA group decreased significantly compared with the MCT group and the MCT+Lactate group, respectively ($p < 0.01$, Fig. 3A, 3C, 3D). indicating DCA treatment alleviated significantly the glycolysis and lactate metabolism in MCT-induced PAH model rats.

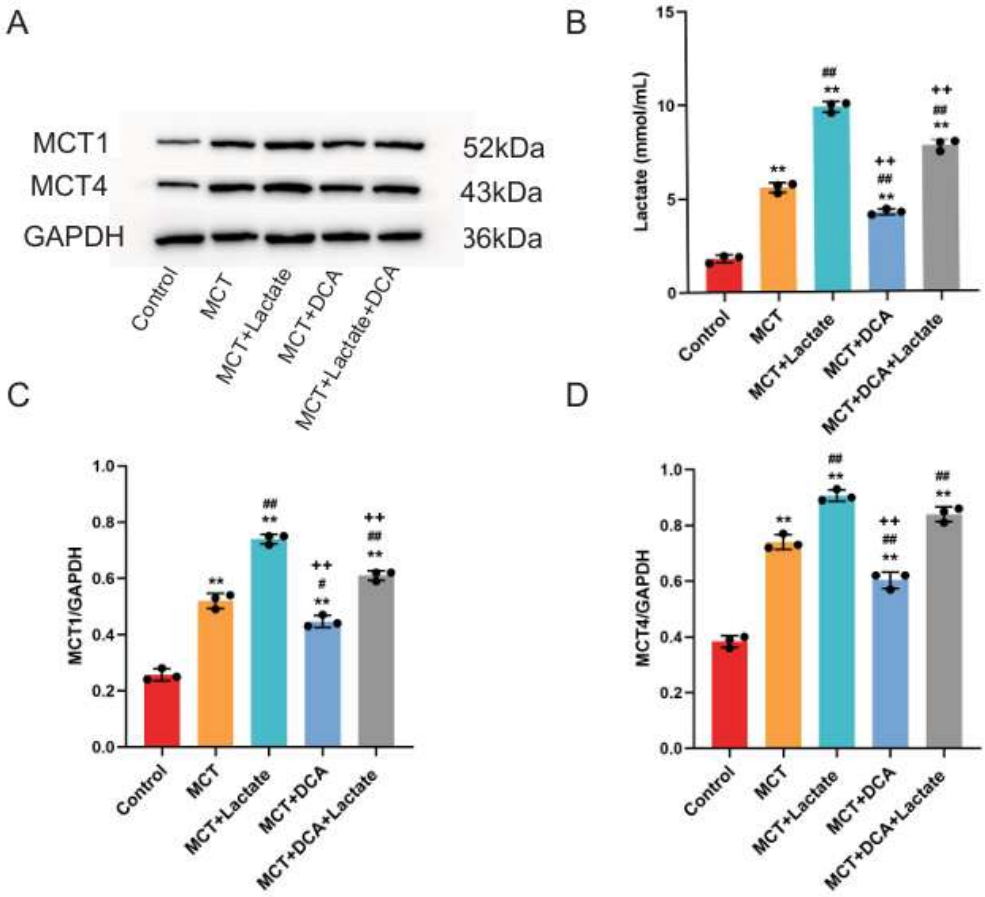


**Figure 3. (A) Representative Western blot bands. (B) The lactate levels quantitative analysis. (C) The expression of MCT1 quantitative analysis. (D) The expression of MCT4 quantitative analysis. *****P*<0.01 vs. control. $^{\#\#}$*P*<0.01 vs. MCT. $^{++}$*P*<0.01 vs. MCT+Lactate; MCT: monocrotaline; MCT1: monocarboxylate transporter 1; MCT4: monocarboxylate transporter 4.**

**Promoted downregulation of H3K18la through HIF-α/PDH-E1α signal blocking may be involved in the remodeling of pulmonary vascular of MCT-induced PAH model rats by DCA.**

the expression of HIF-α and PDH-E1α in MCT+DCA group and MCT+Lactate+DCA group decreased significantly compared with the MCT group and the MCT+Lactate group, respectively ($p < 0.01$, Fig. 4B, 4C). Meanwhile, the expression of H3K18la/HistoneH3 in MCT+DCA group and MCT+Lactate+DCA group decreased significantly compared with the MCT group and the MCT+Lactate group, respectively ($p < 0.01$, Fig. 4D). indicating DCA treatment promoted downregulation of H3K18la through HIF-α/PDH-E1α signal blocking in MCT-induced PAH model rats.

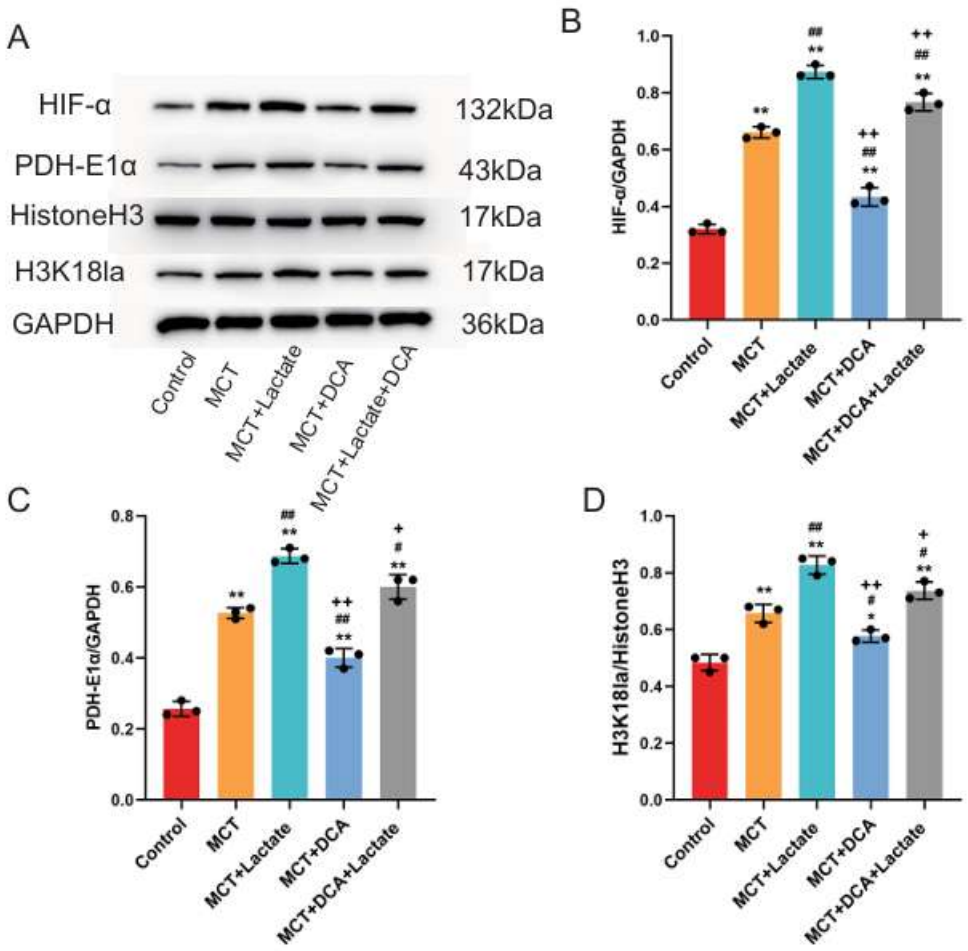


**Figure 4. (A) Representative Western blot bands. (B) The expression of HIF-α quantitative analysis. (C) The expression of PDH-1α quantitative analysis. (D) The expression of H3K18la/HistoneH3 quantitative analysis. **$P$<0.01 vs. control. $^{\#\#}P$<0.01 vs. MCT. $^{++}P$<0.01 vs. MCT+Lactate; MCT: monocrotaline.**

## Discussion

PAH is a progressive vascular disease with a high mortality rate. It is characterized by an occlusive vascular remodeling due to a pro-proliferative and antiapoptotic environment in the wall of resistance pulmonary arteries (PAs) (23, 24). It is increasingly recognized that metabolic abnormalities are not only present in the heart and lungs of PAH patients but are also evident in animal models of the disease(21, 25, 26). Proliferating cells exhibit a cancer-like metabolic switch where mitochondrial glucose oxidation is suppressed, whereas glycolysis is up-regulated as the major source of adenosine triphosphate production. Sharma et al. found that mitochondrial defects and impaired ATP production accelerate lactate production through the Warburg effect, acidifying the tumor microenvironment and promoting cell growth and survival(27). Similar to cancer, The Warburg effect is a contributing factor to PAH, as its characteristic features, such as high glucose uptake, lactate secretion, and anaerobic energy production, are associated with PAH (3, 4). Numerous studies have investigated the relationship between abnormal glucose metabolism and development of PAH to facilitate its treatment.

Notably, in PAH patients, as well as in cell and animal models, there is a shift in glucose metabolism from complete mitochondrial oxidative phosphorylation to increased cytoplasmic glycolysis, leading to the conversion of glucose to pyruvate and ultimately to lactate(28, 29). Michelakis reported that compared to healthy lungs, patients with PAH exhibit increased levels of pyruvate dehydrogenase kinase (PDK), an inhibitor of pyruvate dehydrogenase (PDH). This increase in PDK leads to enhanced glycolysis. Treatment with the PDK inhibitor dichloroacetate activates PDH and increases

mitochondrial respiration, resulting in reduced mean pulmonary artery pressure and pulmonary vascular resistance, thereby improving lung function(30). Interestingly, we observed that DCA treatment not only activates PDH functionally but also reduced the total protein level of its E1α subunit, which was upregulated in the MCT group. This suggests that the chronic glycolytic stress in PAH may induce a compensatory upregulation of total PDH protein, and DCA treatment reverses this pathological change, alongside its primary role as a PDK inhibitor.

Alterations in metabolism and bioenergetics have emerged as common features in both PAH patients and animal models(31). In this study, we focus on the critical role of glycolysis and lactate in the pathogenesis and progression of PAH. Pathological conditions, such as tumors, infections, and ischemia–reperfusion events, facilitate lactate entry into cells via monocarboxylate transporter (MCT). Lactate, a key glycolytic metabolite, is noteworthy for its production even under fully aerobic conditions in cancer cells—a phenomenon termed the Warburg effect.

Historically, lactate was considered a metabolic byproduct, but recent studies have highlighted its role as a donor for the lactylation of histone lysine residues(32). This lactylation can influence epigenetic regulation by promoting chromatin-associated gene transcription, a process known as lactate modification(7). Lactylation significantly impacts inflammation, fibrosis, cellular phenotype transitions, metabolism, aging, and the maintenance of cardiovascular function, demonstrating its unique and profound biological significance(33-36). In the context of tumors, numerous studies indicate that lysine lactylation is associated with the development of hepatocellular carcinoma, colorectal cancer, clear cell renal carcinoma, and ocular melanoma(37-40). PAH shares biological processes with tumors, such as unchecked cell proliferation and resistance to regulatory mechanisms, suggesting that epigenetic dysregulation plays a significant role in PAH development and progression(41). For instance, recent research by Jian Chen and colleagues demonstrated that mitochondrial reactive oxygen species can drive the switch to glycolysis and lactate accumulation in pulmonary artery smooth muscle cells (PASMCs). This, in turn, leads to the lactylation of HIF-1α target proteins and histones, promoting PASMC proliferation and vascular remodeling artery(9, 10). Based on this evidence, we propose that DCA treatment inhibited downregulation of H3K18la through HIF-α/PDH-E1α signal blocking, thus alleviating MCT-induced PAH.

## Footnotes


### Acknowledgments

We thank Glpbio, America, for providing information on the characteristics of DCA. This study was supported by Key Medical Specialty Project of Chengdu,(No.CDS2022Z076); Chengdu Key Clinical Specialty Project (CDS2023ZD002), The College-level project of Chengdu Medical College(CYZYB23-19), Scientific research project of Sichuan Administration of Traditional Chinese Medicine(2023MS177) and Scientific Research Project of Chengdu Science and Technology Bureau (2022-YF05-01459-SN). The funders had no role in the study design, data collection, and analysis, decision to publish, or manuscript preparation.


### Author contributions

Qh. Chen, Jc. He, and Q. Wu designed this work. Qh. Chen, Ml. Chen, and Gq.Jia performed the experiments and drafted the manuscript. Qh. Chen and R. Yin analyzed the data. Qh. Chen, Sj. Bi, Jc. He, and Q. Wu plotted the figures and revised the manuscript. All authors read and approved the final manuscript.

The animal experiments followed the National Institutes of Health Guidelines for the Care and Use of Laboratory Animals and the National Standard of the People's Republic of China for Laboratory Animal Guidelines for Ethical Review of Animal Welfare. This study involving animol tissues strictly adhered to ethical regulations as approved by the Medical Ethics Committee of Chengdu Medical College.


### Corresponding Authors

Correspondence to Qi Wu, E-mail: Wuqi837157@163.com


### Competing Interests

The authors declare no competing interests.

### Data Availability Statement

The data sets used and/or analyzed during the present study are available from the corresponding author upon reasonable request.

**Reference**


1. Warburg O, Wind F, Negelein E. The Metaboli sm of Tumors in the Body. J Gen Physiol. 192 7;8(6):519-30.
2. Vaupel P, Multhoff G. Revisiting the Warburg effect: historical dogma versus current underst anding. J Physiol. 2021;599(6):1745-57.
3. Ryanto GRT, Suraya R, Nagano T. Mitochondr ial Dysfunction in Pulmonary Hypertension. A ntioxidants (Basel). 2023;12(2).
4. Arai MA, Sakuraba K, Makita Y, Hara Y, Ishib ashi M. Evaluation of Naturally Occurring HI F-1 Inhibitors for Pulmonary Arterial Hyperte nsion. Chembiochem. 2021;22(18):2799-804.
5. Bhagat TD, Von Ahrens D, Dawlaty M, et al. Lactate-mediated epigenetic reprogramming r egulates formation of human pancreatic cancer -associated fibroblasts. Elife. 2019;8.
6. Zhang N, Jiang N, Yu L, et al. Protein Lactylat ion Critically Regulates Energy Metabolism in the Protozoan Parasite Trypanosoma brucei. Fr ont Cell Dev Biol. 2021;9:719720.
7. Zhang D, Tang Z, Huang H, et al. Metabolic re gulation of gene expression by histone lactylat ion. Nature. 2019;574(7779):575-80.
8. Stillman B. Histone Modifications: Insights int o Their Influence on Gene Expression. Cell. 2 018;175(1):6-9.
9. Xiao Y, Peng H, Hong C, et al. PDGF Promote s the Warburg Effect in Pulmonary Arterial Sm ooth Muscle Cells via Activation of the PI3K/ AKT/mTOR/HIF-1alpha Signaling Pathway. Cell Physiol Biochem. 2017;42(4):1603-13.
10. Chen J, Zhang M, Liu Y, et al. Histone lactylat ion driven by mROS-mediated glycolytic shift promotes hypoxic pulmonary hypertension. J Mol Cell Biol. 2023;14(12).
11. Jin AH, Qian YF, Ren J, et al. PDK inhibition promotes glucose utilization, reduces hepatic l ipid deposition, and improves oxidative stress in largemouth bass (Micropterus salmoides) b y increasing pyruvate oxidative phosphorylati on. Fish Shellfish Immunol. 2023;140:108969.
12. Rajabi S, Najafipour H, Jafarinejad Farsangi S, et al. Perillyle alcohol and Quercetin amelio rate monocrotaline-induced pulmonary artery hypertension in rats through PARP1-mediated miR-204 down-regulation and its downstream pathway. BMC Complement Med Ther. 2020; 20(1):218.
13. Cao N, Tang X, Gao R, et al. Galectin-3 partic ipates in PASMC migration and proliferation b y interacting with TGF-beta1. Life Sci. 2021;2 74:119347.
14. Zhao X, Bai X, Li JL, Li SM, Xi J. Sevofluran e improves circulatory function and pulmonar y fibrosis in rats with pulmonary arterial hyper tension through inhibiting NF-kappaB signalin g pathway. Eur Rev Med Pharmacol Sci. 201 9;23(23):10532-40.
15. Urboniene D, Haber I, Fang YH, Thenappan T, Archer SL. Validation of high-resolution ec hocardiography and magnetic resonance imagi ng vs. high-fidelity catheterization in experime ntal pulmonary hypertension. Am J Physiol Lu ng Cell Mol Physiol. 2010;299(3):L401-12.
16. Zaky A, Zafar I, Masjoan-Juncos JX, et al. Ec hocardiographic, Biochemical, and Electrocar diographic Correlates Associated With Progres sive Pulmonary Arterial Hypertension. Front C ardiovasc Med. 2021;8:705666.
17. Luan Y, Chao S, Ju ZY, et al. Therapeutic effe cts of baicalin on monocrotaline-induced pulm onary arterial hypertension by inhibiting infla mmatory response. Int Immunopharmacol. 20 15;26(1):188-93.
18. Chen M, Ding Z, Zhang F, et al. A20 attenuate s hypoxia-induced pulmonary arterial hyperten sion by inhibiting NF-kappaB activation and p ulmonary artery smooth muscle cell proliferati on. Exp Cell Res. 2020;390(2):111982.
19. Luo L, Wu J, Lin T, et al. Influence of atorvast atin on metabolic pattern of rats with pulmona ry hypertension. Aging (Albany NY). 2021;13 (8):11954-68.
20. Cao Y, Zhang X, Wang L, et al. PFKFB3-medi ated endothelial glycolysis promotes pulmonar y hypertension. Proc Natl Acad Sci U S A. 201 9;116(27):13394-403.
21. Hernandez-Saavedra D, Sanders L, Freeman S, et al. Stable isotope metabolomics of pulmo nary artery smooth muscle and endothelial cell s in pulmonary hypertension and with TGF-be ta treatment. Sci Rep. 2020;10(1):413.
22. Singh M, Afonso J, Sharma D, et al. Targeting monocarboxylate transporters (MCTs) in canc er: How close are we to the clinics? Semin Ca ncer Biol. 2023;90:1-14.
23. Hassoun PM. Pulmonary Arterial Hypertensio n. The New England journal of medicine. 202

1;385(25):2361-76.
24. Ruopp NF, Cockrill BA. Diagnosis and Treat ment of Pulmonary Arterial Hypertension: A R eview. Jama. 2022;327(14):1379-91.
25. Xu W, Erzurum SC. Endothelial cell energy m etabolism, proliferation, and apoptosis in pulm onary hypertension. Comprehensive Physiolog y. 2011;1(1):357-72.
26. Xu W, Comhair SAA, Chen R, et al. Integrativ e proteomics and phosphoproteomics in pulmo nary arterial hypertension. Sci Rep. 2019;9(1): 18623.
27. Sharma NK, Pal JK. Metabolic Ink Lactate M odulates Epigenomic Landscape: A Concerted Role of Pro-tumor Microenvironment and Ma croenvironment During Carcinogenesis. Curr Mol Med. 2021;21(3):177-81.
28. Drake JI, Bogaard HJ, Mizuno S, et al. Molec ular signature of a right heart failure program i n chronic severe pulmonary hypertension. Am erican journal of respiratory cell and molecula r biology. 2011;45(6):1239-47.
29. Zhao L, Ashek A, Wang L, et al. Heterogeneit y in lung (18)FDG uptake in pulmonary arteri al hypertension: potential of dynamic (18)FD G positron emission tomography with kinetic analysis as a bridging biomarker for pulmonar y vascular remodeling targeted treatments. Cir culation. 2013;128(11):1214-24.
30. Michelakis ED, Gurtu V, Webster L, et al. Inhi bition of pyruvate dehydrogenase kinase impr oves pulmonary arterial hypertension in geneti cally susceptible patients. Sci Transl Med. 201 7;9(413).
31. Xu W, Janocha AJ, Erzurum SC. Metabolism i n Pulmonary Hypertension. Annual review of physiology. 2021;83:551-76.
32. Morgan MAJ, Shilatifard A. Reevaluating the roles of histone-modifying enzymes and their associated chromatin modifications in transcri ptional regulation. Nature genetics. 2020;52(1 2):1271-81.
33. Moreno-Yruela C, Zhang D, Wei W, et al. Clas s I histone deacetylases (HDAC1-3) are histon e lysine delactylases. Sci Adv. 2022;8(3):eabi6 696.
34. Chen H, Li Y, Li H, et al. NBS1 lactylation is r equired for efficient DNA repair and chemothe rapy resistance. Nature. 2024;631(8021):663- 9.
35. Chen Y, Wu J, Zhai L, et al. Metabolic regulati on of homologous recombination repair by M RE11 lactylation. Cell. 2024;187(2):294-311 e 21.
36. Cheng X, Wang K, Zhao Y, Wang K. Research progress on post-translational modification of proteins and cardiovascular diseases. Cell Dea th Discov. 2023;9(1):275.
37. Miao Z, Zhao X, Liu X. Hypoxia induced beta -catenin lactylation promotes the cell prolifera tion and stemness of colorectal cancer through the wnt signaling pathway. Exp Cell Res. 202 3;422(1):113439.
38. Yang J, Luo L, Zhao C, et al. A Positive Feedb ack Loop between Inactive VHL-Triggered Hi stone Lactylation and PDGFRbeta Signaling Drives Clear Cell Renal Cell Carcinoma Progr ession. Int J Biol Sci. 2022;18(8):3470-83.
39. Yao G, Yang Z. Glypican-3 knockdown inhibit s the cell growth, stemness, and glycolysis dev elopment of hepatocellular carcinoma cells un der hypoxic microenvironment through lactyla tion. Arch Physiol Biochem. 2024;130(5):546- 54.
40. Yu J, Chai P, Xie M, et al. Histone lactylation drives oncogenesis by facilitating m(6)A reade r protein YTHDF2 expression in ocular melan oma. Genome Biol. 2021;22(1):85.
41. Galiè N, McLaughlin VV, Rubin LJ, Simonne au G. An overview of the 6th World Symposiu m on Pulmonary Hypertension. The European respiratory journal. 2019;53(1).